Advanced Nano-Bio-Materials and Devices - AdvNanoBioM&D Open Acces Journal
powered by SciEdTech

Ab Initio Study of Heme Complex as a Nano-Biosensor for CO and O_2 Gases

Amir HADADI*[1], Ali REZAEI BOLVERDI[2], Morteza JAMSHIDI[2], Omid REZAEI[2]

[1]Department of Electronic, Kermanshah Branch, Islamic Azad University, Kermanshah, Iran

[2]Young Researchers and Elite Club, Kermanshah Branch, Islamic Azad University, Kermanshah, Iran

Abstract

Heme-based Metalloproteins play essential part as nano-biosensor for diatomic gases such as NO, O_2, CO and so on. The electron and optic properties, and adsorption energy of Heme complex as the nano-biosensor for O_2 and CO gases were studied using ab initio studies and density function theory (DFT) approach. The results show that Heme is highly capable of being used as a nano-biosensor for O_2 and CO gases. Carbon monoxide has a lower adsorption energy but higher electron transfers with Heme. Energy gap raised to 0.09 eV in the presence of O_2 and to 0.39 Ev in the presence of CO, which indicates the higher sensitivity of Heme to CO.

Keywords: *Ab Initio, Nano-Biosensor, Carbon monoxide, Heme*

1. Introduction

Iron-containing enzymes (Hemes) contribute greatly to the adsorption of oxygen in biological systems due to their active sites [1, 2]. For instance, Heme helps to transfer oxygen to different parts of the body as a carrier of O_2 in hemoglobins. The O_2 is restored in cytochrome [3-6]. Numerous studies have been done to identify the structure of this complex and its reaction stages with oxygen and other biogases [7-11]. Based on the data obtained on the possible structures of the Heme crystals, this complex is made up of a ligand, four crown like teeth with a Porphyrin base and one oxygen atom. It possesses a conjugated electron system [12-15] (Figure 1). Prior to the Heme reaction with oxygen, the coordination number of Fe(III) (ferric) that changes into Fe(II) (ferrous) for reaction, then the oxygen adsorption mechanism of this enzyme will be start [16-18]. Hence, the existence of such active sites on Heme like ferric, and its abundance and high biocompatibility enables us to design and produce Heme-based O_2, CO, and CO_2 biosensors [19, 20].

Heme proteins include a great variety of interaction with diatomic gas ligands, anions and bases. A great number of Heme proteins have been identified as a basis for sensing diatomic ligands such as O_2, CO, and NO in the past two decades [21-23]. It has been proved that the structure of Heme protein can be effective on the bonding capability of ligands with the Heme group. The bonding strength of CO_2 with Heme free in solution is $2*10^4$ as much as that of oxygen whereas the myoglobin of this factor decreases 25 times [16, 24].

In 2005, Andrea Decker and Edward I Solomon carried out calculations on the oxygen adsorption mechanism of iron-containing Heme and iron-free Heme using DFT (density functional theory) approach. In the iron-free Heme version, iron was replaced with copper. They concluded that the oxygen adsorption mechanism is totally different in these two states. They asserted that the adsorption

mechanism of dioxygen on Heme depended on the metal present in its structure [25].

Thomas G. Spiro and Andrzej A. Jarzecki (2005) studied the reaction between X-O (X=O, N, C) using DFT approach. They concluded that each of these diatomic gases interacts with each other in a different angle [26].

In this study, the Heme complex with a structure as in Figure 1 was used as a nano-biosensor for the detection of two diatomic O_2 and CO gases. So, DFT calculation method, and effective core potentials basis sets were used to obtain structural, electron, and optic data, and to compare the data related to each gas.

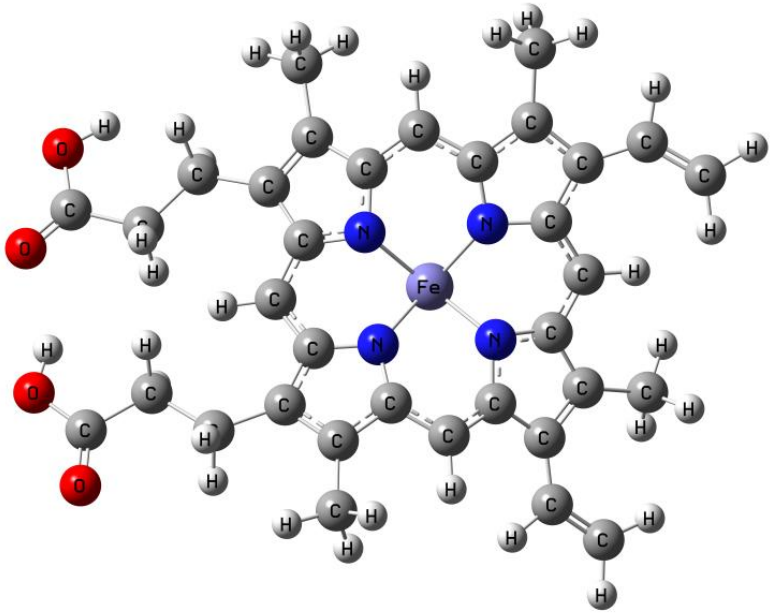

Figure1. The structure of Heme containing Fe

2. Computational details

In this work, the sensing effect of the Heme complex on diatomic CO and O_2 gases was studied. All the calculations were done using a Gaussian 03 software package. It should be noted that all the calculations were done in a 298.15 Kelvin temperature with a pressure of one atmosphere in a gaseous phase. First, the structure of Heme complex [27] (Figure 1) was optimized using DFT approach and B3LYP/lanl2dz basis set [28-30]. In order to identify the optimal distance of CO and O_2 (in both states) from Heme complex [31, 32], and to obtain the structure energy, in different distances from 2.2 to 4.2 angstroms were studied [33, 34]. Figure 2 shows the energy graph in terms of distance for CO and O_2 CO has approached the Heme complex from two sides; once from oxygen and the other from carbon atom. The optimal distance 3.6 A^0 was obtained for O_2. When CO approaches the Heme complex from O, the optimal distance is 2.8 A^0 but when it approaches from C, the optimal distance is 3.4Ä.

NBO (natural bond orbital) analysis [35, 36], optic, and electron calculations for the optimal distances were done using the same previous approach and basis set. The data related to the orbital geometry, and the UV-Vis and DOS (density of state) spectrums were obtained. The DOS spectrum data were extracted using the Gausssum 3.0 software.

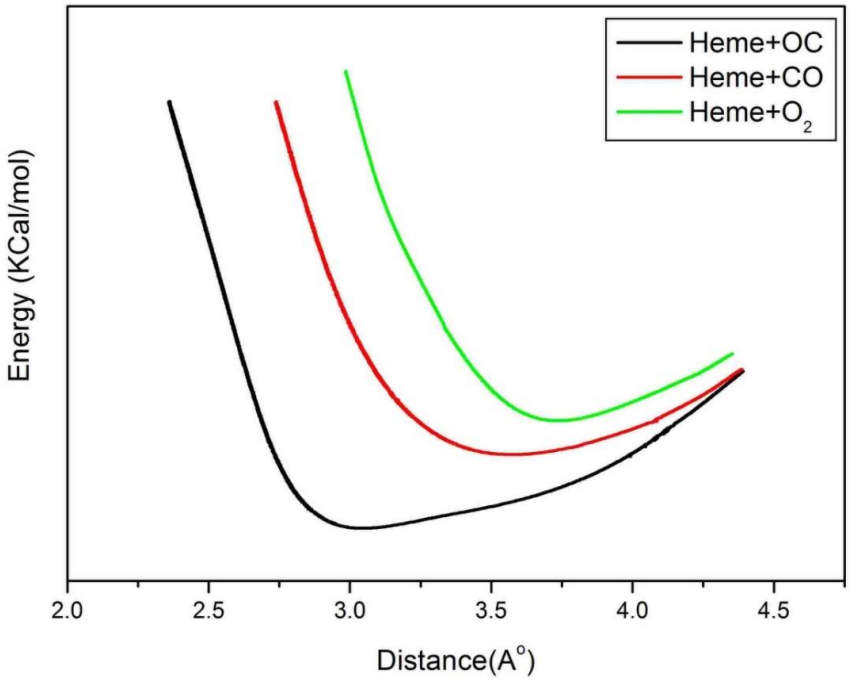

Fig.2 the graph of optimal energy in terms of the distance of CO and O_2 gases from the Heme Complex

3. Result and Discussion

3.1. Electron transfers analysis

Electron transfers from C-N bonds and nitrogen electron pairs of the Porphyrin ring to Fe are presented in Table 1. Electron transfers from nitrogen electron pairs possess greater values[37]. For instance, the transfer $\sigma C_3N_4 \rightarrow LP^*_{(6)}$ Fe has the value of 2.64 Kcal/mol while the transfer $LP_{(1)} N_{21} \rightarrow LP^*_{(5)}$ Fe has the value of 47.10 Kcal/mol. After the addition of CO and O_2, the amount of these transfers has been considerably lowered (Table 2). That's because CO and O_2 exchange electrons with the Fe atom. This lowers the Fe tendency to receive electron from nitrogen pair electrons in the porphyrin ring. Decrease in electron transfers from nitrogen electron pairs in the presence of CO is a bit greater than O_2 because CO has greater tendency towards Heme. Carbon monoxide has approached Heme from both C and O heads. A small difference is observed for these two states. Moreover, electron transfers from CO and O_2 to iron are presented in Table 2. Most of these transfers are small but among these transfers, transfers from O electron pairs in dioxygen, and C and O in CO have greater values. For instance, the transfer $LP_{(1)} O_{73} \rightarrow LP^*_{(8)}$ Fe is 8.37 kcal/mol when CO approaches Heme from O but the transfer $LP_{(1)} C_{74} \rightarrow LP^*_{(8)}$ Fe is 6.14 kcal/mol when CO approaches Heme from C. It can be easily seen that the electron transfer from CO is greater than that of O_2 in both states.

In Figure 4, the images of HOMO and LUMO orbitals are shown in both the presence and absence of CO and O_2. HOMO and LUMO energy, energy gap, adsorption energy, and Muliken Charge are given in Table 3. The frontal orbitals of LUMO in the Heme complex have focused on Fe since the 3d orbitals of Fe are free. These extensive LUMO cause the Fe to be ready to receive electron from electronegative ligands. After the addition of CO and O_2 ligands, the frontal orbitals of LUMO are found on the surface of Heme not on Fe, which indicates electron transfer to Fe

and a decrease in its tendency to receive electrons. The energy level of HOMO has the constant value of -5.5 e V both after and before the addition of CO and O_2 gases. Since the HOMO orbitals do not have an effect on the physical adsorption of these gases, HOMO energy level does not undergo a change whereas the LUMO energy level increases after the physical adsorption of gases.

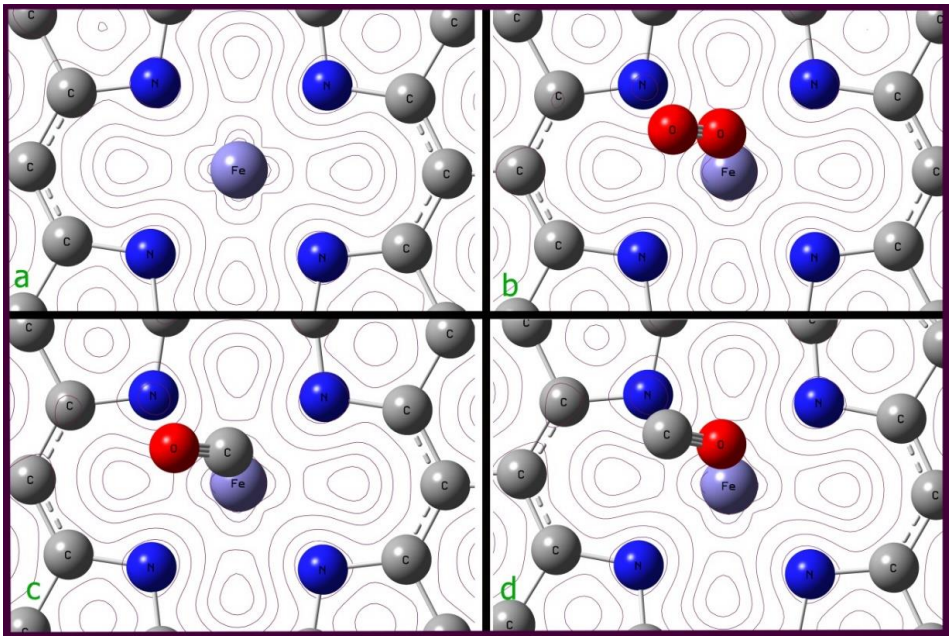

Figure 3. Electron density gradient: a) Heme Complex b) Heme +O_2 c) Heme + CO d) Heme + OC

Table 1. Electron transfers from porphyrin ring to Fe

	Electron transfer			
	Hem	Hem+O_2	Hem+CO	Hem+OC
$\sigma C_3N_4 \rightarrow LP^*_{(6)}$ Fe	5.89	1.91	3.62	5.46
$\sigma C_3N_4 \rightarrow LP^*_{(8)}$ Fe	3.09	-	0.20	2.89
$\sigma C_5N_4 \rightarrow LP^*_{(6)}$ Fe	5.70	1.18	4.79	6.30
$\sigma c_8N_9 \rightarrow LP^*_{(7)}$ Fe	5.88	1.90	3.80	5.73
$\sigma c_8N_9 \rightarrow LP^*_{(8)}$ Fe	3.08	0.05	2.85	2.72
$\sigma c_{10}N_9 \rightarrow LP^*_{(7)}$ Fe	5.70	1.17	5.03	6.56
$\sigma c_{14}N_{15} \rightarrow LP^*_{(6)}$ Fe	5.86	1.93	3.68	5.49
LP $_{(1)}$ $N_4 \rightarrow LP^*_{(5)}$ Fe	47.81	23.07	46.34	46.93
LP $_{(1)}$ $N_9 \rightarrow LP^*_{(4)}$ Fe	44.87	22.31	44.87	45.18
LP $_{(1)}$ $N_{15} \rightarrow LP^*_{(5)}$ Fe	46.78	23.18	42.94	43.89
LP $_{(1)}$ $N_{21} \rightarrow LP^*_{(5)}$ Fe	47.10	23.60	45.08	45.71

Table.2 Electron transfers from CO and O_2 gases to Fe

Electron transfer				
	CO	OC		O_2
$\pi CO \rightarrow LP^*_{(6)}$ Fe	-	0.19	$\sigma O_2 \rightarrow LP^*_{(8)}$ Fe	0.04
$\pi CO \rightarrow LP^*_{(7)}$ Fe	-	0.06	$\pi O_2 \rightarrow LP^*_{(7)}$ Fe	0.05
$\pi CO \rightarrow LP^*_{(8)}$ Fe	0.21	0.12	-	-
$\pi CO \rightarrow LP^*_{(9)}$ Fe	-	0.24	-	-
$\pi_2 CO \rightarrow LP^*_{(5)}$ Fe	-	0.05	-	-
$\pi_2 CO \rightarrow LP^*_{(7)}$ Fe	0.07	0.07	-	-
$\pi_2 CO \rightarrow LP^*_{(8)}$ Fe	-	1.91	-	-
$\pi_2 CO \rightarrow LP^*_{(9)}$ Fe	0.03	-	-	-
$LP_{(1)} O_{73} \rightarrow LP^*_{(5)}$ Fe	-	0.65	$LP_{(1)} O_{73} \rightarrow LP^*_{(5)}$ Fe	0.13
$LP_{(1)} O_{73} \rightarrow LP^*_{(6)}$ Fe	-	0.11	$LP_{(1)} O_{73} \rightarrow LP^*_{(6)}$ Fe	0.03
$LP_{(1)} O_{73} \rightarrow LP^*_{(7)}$ Fe	-	0.22	$LP_{(1)} O_{73} \rightarrow LP^*_{(8)}$ Fe	1.19
$LP_{(1)} O_{73} \rightarrow LP^*_{(8)}$ Fe	-	8.37	$LP_{(2)} O_{73} \rightarrow LP^*_{(5)}$ Fe	0.07
$LP_{(1)} O_{73} \rightarrow LP^*_{(9)}$ Fe	-	0.67	$LP_{(2)} O_{73} \rightarrow LP^*_{(6)}$ Fe	0.08
$LP_{(1)} C_{74} \rightarrow LP^*_{(5)}$ Fe	1.25	0.41	$LP_{(2)} O_{73} \rightarrow LP^*_{(8)}$ Fe	0.46
$LP_{(1)} C_{74} \rightarrow LP^*_{(6)}$ Fe	0.35	0.11	$LP_{(1)} O_{74} \rightarrow LP^*_{(5)}$ Fe	0.03
$LP_{(1)} C_{74} \rightarrow LP^*_{(7)}$ Fe	0.09	-	$LP_{(1)} O_{74} \rightarrow LP^*_{(8)}$ Fe	0.07
$LP_{(1)} C_{74} \rightarrow LP^*_{(8)}$ Fe	6.14	1.29	$LP_{(2)} O_{74} \rightarrow LP^*_{(6)}$ Fe	0.04
$LP_{(1)} C_{74} \rightarrow LP^*_{(9)}$ Fe	0.78	0.22	$LP_{(2)} O_{74} \rightarrow LP^*_{(8)}$ Fe	0.04

Table 3. Energy of HOMO and LUMO, energy of adsorption and Muliken charge

	E_{HOMO}	E_{LUMO}	E_g	ΔE_g	E_{ads}	MC_{Fe}
Heme	-5.5	-0.37	5.13	0	-	0.624
Heme+O_2	-5.5	-0.28	5.22	0.09	45.23	0.971
Heme+CO	-5.5	0.02	5.52	0.39	23.67	0.966
Heme+OC	-5.5	0.02	5.52	0.39	21.41	0.978

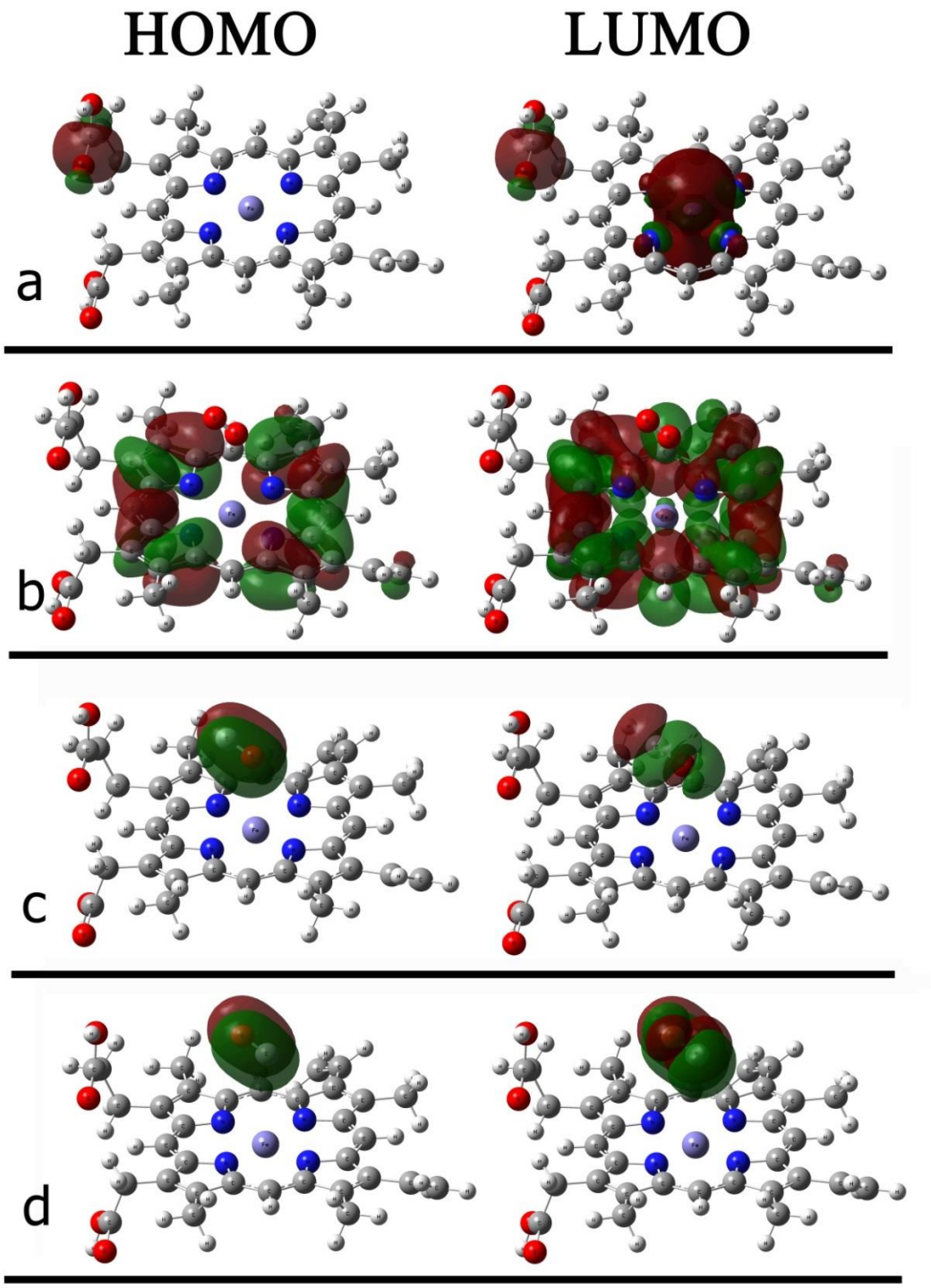

Figure 4. The images of HOMO and LUMO orbitals: a) Heme complex b) Heme+O2 c) Heme+OC d) Heme+CO

We get the adsorption energy from the Eq 1 [38]:

$$E_{Ads}=E\,(Heme+gas)-E_{HEM}-E_{gas} \quad (1)$$

This shows that the adsorption energy for CO is lower than O_2, and that adsorption energy for CO is lower than O. Mulliken charge [39] has remarkably increased on the Fe atom subsequent to the gas adsorption on Heme. This is because of electron transfer from gas to the Fe atom.

Figure 5 shows the DOS diagram of the Heme complex both in the presence and absence of CO and O_2 gases. The gap energy for the Heme complex is 5.13 e V while it rises to 5.22 eV in the presence of dioxygen, and to 5.52 e V in the presence of CO. As for the NBO data available, a greater change in energy gap was expected in the presence of CO. The Heme complex can be easily used to detect CO and O_2 gases via this gap energy change. Moreover, with the greater change in gap energy in the presence of CO, the Heme complex becomes more sensitive to CO.

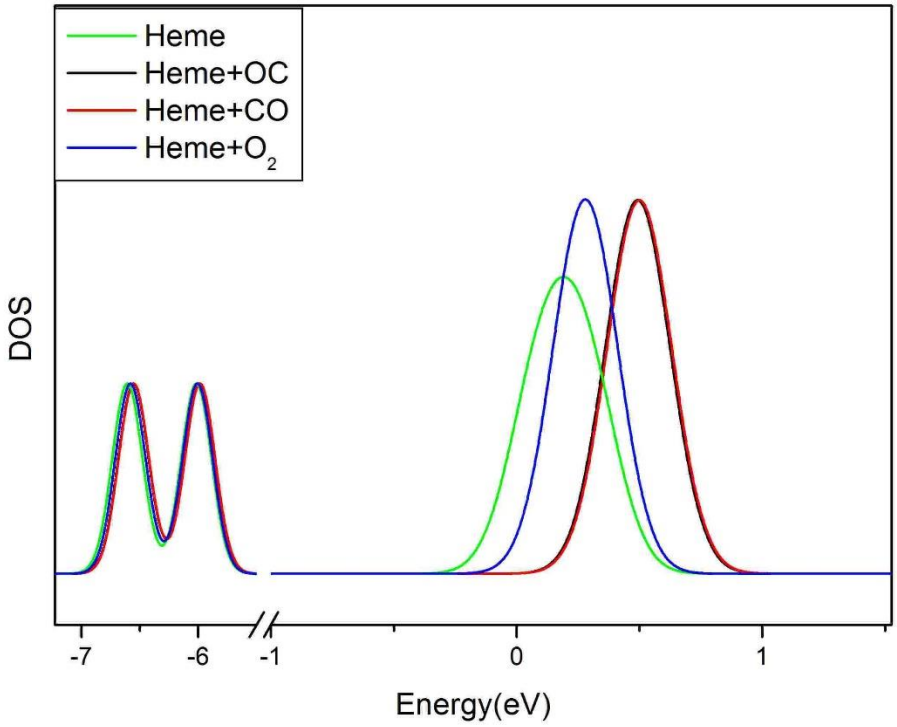

Figure 5. The density of states (DOS) diagram of the Heme complex before and after the adition of CO and O_2 gases

3.2. Optical investigations

The UV-Vis of Heme in the presence and absence of is given in the Figure 6. The conjugated structure of Heme complex displays a maximum peak in the region of 313 nm Which is a result of π electron transfers to the conjugated complex π* bonds. The maximum peak moves toward higher wavelengths in the presence of CO and O_2. Additionally, the intensity of this peak has decreased. Such changes occur more in the presence of O_2. The changes in the maximum peak are the same in the presence of CO, namely, whether it approaches the Heme complex from C or from O. The very same trend is seen in electron transfers illustrated by NBO data.

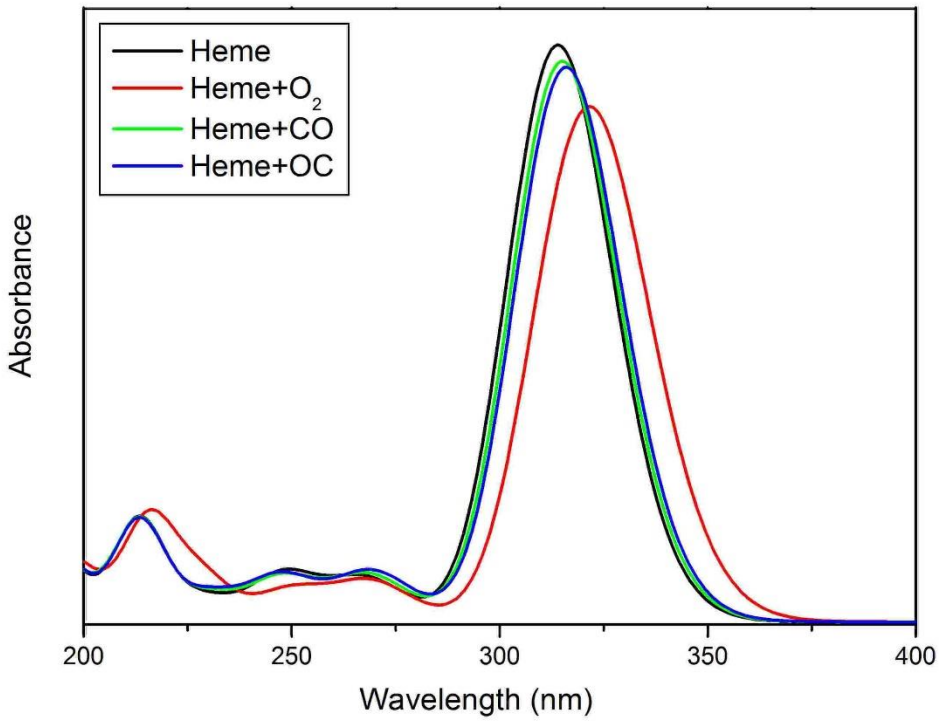

Figure 6. The UV-Vis adsorptive spectrum of the Heme complex before and after the addition O_2 and CO

4. Conclusion

The Heme complex was studied as a nano-biosensor for the CO and O_2 gases. The NBO data displayed a clear difference in electron transfers in the presence and absence of these gases. After the addition of the gases, electron transfers from Porphyrin ring decreased remarkably. This finding is also supported by electron density calculations. These changes make the density of states different and raise the energy gap to 0.09 eV in the presence of O_2 and to 0.39 eV in the presence of CO. This energy gap change can be used as an electrochemical nano-biosensor for the CO and O_2 gases. The maximum wavelength and intensity of Heme complex UV-Vis spectrum have changed subsequent to the addition of these gases; the intensity of maximum peak has decreased and moved towards higher wavelengths. These changes can be used as a suitable optical sensor for the detection of these gases. Due to the good results obtained from this nano-bio-sensors, it can be an efficient Heme-based sensor manufacturing.

Refrences

[1] Gilles-Gonzalez M-A, Gonzalez G. Heme-based sensors: defining characteristics, recent developments, and regulatory hypotheses. Journal of Inorganic Biochemistry. 2005;99(1):1-22.

[2] Neubauer JA, Sunderram J. Heme oxygenase-1 and chronic hypoxia. Respiratory Physiology & Neurobiology. 2012;184(2):178-85.

[3] Gray HB. Biological inorganic chemistry at the beginning of the 21st century. Proceedings of the National Academy of Sciences. 2003;100(7):3563-8.

[4] Hirotsu S, Chu GC, Unno M, Lee D-S, Yoshida T, *et al.* The crystal structures of the ferric and ferrous forms of the heme complex of HmuO, a heme oxygenase of Corynebacterium

diphtheriae. Journal of Biological Chemistry. 2004;279(12):11937-47.

[5] Berg JM, Tymoczko JL, Stryer L. Protein structure and function. 2002.

[6] Babcock GT, Varotsis C. Discrete steps in dioxygen activation - The cytochrome oxidase/ O_2 reaction. Journal of bioenergetics and biomembranes. 1993;25(2):71-80.

[7] Kovaleva EG, Lipscomb JD. Versatility of biological non-heme Fe(II) centers in oxygen activation reactions. Nature chemical biology. 2008;4(3):186-93.

[8] Autenrieth F, Tajkhorshid E, Baudry J, Luthey-Schulten Z. Classical force field parameters for the heme prosthetic group of cytochrome c. Journal of computational chemistry. 2004; 25(13): 1613-22.

[9] Park J, Morimoto Y, Lee Y-M, Nam W, Fukuzumi S. Metal Ion Effect on the Switch of Mechanism from Direct Oxygen Transfer to Metal Ion-Coupled Electron Transfer in the Sulfoxidation of Thioanisoles by a Non-Heme Iron (IV) − Oxo Complex. Journal of the American Chemical Society. 2011;133(14): 5236-9.

[10] Shimizu T, Huang D, Yan F, Stranava M, Bartosova M*, et al.* Gaseous O_2, NO, and CO in Signal Transduction: Structure and Function Relationships of Heme-Based Gas Sensors and Heme-Redox Sensors. Chemical Reviews. 2015;115(13):6491–6533.

[11] Kaewruksa B, Pipornpong W, Wanno B, Ruangpornvisuti V. Density functional studies of small gases adsorbed on the ZnO sodalite-like cage and its adsorption abilities. Computational and Theoretical Chemistry. 2013;1020:100-7.

[12] Dolphin D. The Porphyrins V7: Biochemistry: Elsevier; 2012.

[13] Severance S, Hamza I. Trafficking of heme and porphyrins in metazoa. Chemical reviews. 2009;109(10):4596-616.

[14] Ishitsuka Y, Araki Y, Tanaka A, Igarashi J, Ito O*, et al.* Arg97 at the Heme-Distal Side of the Isolated Heme-Bound PAS Domain of a Heme-Based Oxygen Sensor from Escherichia coli (Ec DOS) Plays Critical Roles in Autoxidation and Binding to Gases, Particularly O_2. Biochemistry. 2008;47(34):8874-84.

[15] Goldberg MA, Dunning SP, Bunn HF. Regulation of the erythropoietin gene: evidence that the oxygen sensor is a heme protein. Science. 1988;242(4884):1412-5.

[16] Schuller DJ, Wilks A, de Montellano PRO, Poulos TL. Crystal structure of human heme oxygenase-1. Nature Structural & Molecular Biology. 1999;6(9):860-7.

[17] Paulat F, Lehnert N. Electronic structure of ferric heme nitrosyl complexes with thiolate coordination. Inorganic Chemistry. 2007;46(5): 1547-9.

[18] Ortiz de Montellano PR. Heme oxygenase mechanism: evidence for an electrophilic, ferric peroxide species. Accounts of chemical research. 1998;31(9):543-9.

[19] Marvin KA, Reinking JL, Lee AJ, Pardee K, Krause HM*, et al.* Nuclear receptors Homo sapiens Rev-erbβ and Drosophila melanogaster E75 are thiolate-ligated heme proteins which undergo redox-mediated ligand switching and bind CO and NO. Biochemistry. 2009;48(29): 7056-71.

[20] Dong X, Fu D, Ahmed MO, Shi Y, Mhaisalkar S*, et al.* Heme-enabled electrical detection of carbon monoxide at room temperature using networked carbon nanotube field-effect transistors. Chemistry of Materials. 2007; 19(25): 6059-61.

[21] Abdurahman A, Renger T. Density functional studies of iron-porphyrin cation with small ligands X (X: O, CO, NO, O_2, N_2, H_2O, N_2O, CO_2). The Journal of Physical Chemistry A. 2009;113(32):9202-6.

[22] Daskalakis V, Varotsis C. Binding and docking interactions of NO, CO and O_2 in heme proteins as probed by density functional theory. International journal of molecular sciences. 2009;10(9):4137-56.

[23] Fabris S, Stepanow S, Lin N, Gambardella P, Dmitriev A*, et al.* Oxygen dissociation by concerted action of di-iron centers in metal–organic coordination networks at surfaces: modeling non-heme iron enzymes. Nano letters. 2011;11(12):5414-20.

[24] Tuckey RC, Kamin H. Kinetics of O_2 and CO Binding to adrenal cytochrome P-450scc. Effect of cholesterol, intermediates, and phosphatidylcholine vesicles. Journal of Biological Chemistry. 1983;258(7):4232-7.

[25] Decker A, Solomon EI. Dioxygen activation by copper, heme and non-heme iron enzymes: comparison of electronic structures and reactivities. Current opinion in chemical biology. 2005;9(2):152-63.

[26] Spiro TG, Jarzecki AA. Heme-based sensors: theoretical modeling of heme-ligand–protein interactions. Current opinion in chemical biology. 2001;5(6):715-23.

[27] Park H, Suquet C, Satterlee JD, Kang C. Insights into signal transduction involving PAS domain oxygen-sensing heme proteins from the X-ray crystal structure of Escherichia coli Dos heme domain (Ec DosH). Biochemistry. 2004;43(10):2738-46.

[28] Nagarajan V, Chandiramouli R. TeO_2 nanostructures as a NO_2 sensor: DFT investigation. Computational and Theoretical Chemistry. 2014;1049:20-7.

[29] Li L, Li M, Wang X, Wang Q. Density functional theory study on the “Molecular Taekwondo” process of pyrene-armed calix-[4]-azacrowns. Computational and Theoretical Chemistry. 2014;1031:40-9.

[30] Jamshidi M, Rezaei O, Belverdi AR, Malekian S, Belverdi AR. A highly selective fluorescent chemosensor for Mg^{2+} ion in aqueous solution using density function theory calculations. Journal of Molecular Structure. 2016;1123:111-5.

[31] Sainna MA, Kumar S, Kumar D, Fornarini S, Crestoni ME*, et al.* A comprehensive test set of epoxidation rate constants for iron (IV)–oxo porphyrin cation radical complexes. Chemical Science. 2015;6(2):1516-29.

[32] He Y, Zhang J, Zhao J. Theoretical Investigation on the Electronic Transport Properties of Iron(II) Porphyrin for CO Sensing with Single-walled Carbon Nanotubes. Chemistry Letters. 2014;43(5):735-7.

[33] Zhang H-P, Luo X-G, Song H-T, Lin X-Y, Lu X*, et al.* DFT study of adsorption and dissociation behavior of H_2S on Fe-doped graphene. Applied Surface Science. 2014;317:511-6.

[34] Seyed-Talebi SM, Beheshtian J. Computational study of ammonia adsorption on the perfect and rippled graphene sheet. Physica B: Condensed Matter. 2013;429:52-6.

[35] Choudhary N, Bee S, Gupta A, Tandon P. Comparative vibrational spectroscopic studies, HOMO–LUMO and NBO analysis of N-(phenyl)-2,2-dichloroacetamide, N-(2-chloro phenyl)-2,2-dichloroacetamide and N-(4-chloro phenyl)-2,2-dichloroacetamide based on density functional theory. Computational and Theoretical Chemistry. 2013;1016:8-21.

[36] Bilal S, Bibi S, Ahmad SM, Shah A-u-HA. Counterpoise-corrected energies, NBO, HOMO–LUMO and interaction energies of poly(o-aminophenol) for ammonia sensing by DFT methods. Synthetic Metals. 2015;209:143-9.

[37] Tavakol H, Mollaei-Renani A. DFT, AIM, and NBO study of the interaction of simple and sulfur-doped graphenes with molecular halogens, CH_3OH, CH_3SH, H_2O, and H_2S. Structural Chemistry. 2014;25(6):1659-67.

[38] Yang W-H, Lu W-C, Xue X-Y, Zang Q-J. A theoretical study on CO sensing mechanism of In-doped SnO_2 (1 1 0) surface. Computational and Theoretical Chemistry. 2015;1069:119-124.

[39] Tsuneyuki S, Tsukada M, Aoki H, Matsui Y. First-principles interatomic potential of silica applied to molecular dynamics. Physical review letters. 1988;61(7):869.